



Synthesis, *in silico*, *in vitro* and *in vivo* evaluations of isatin aroylhydrazones as highly potent anticonvulsant agents

Saeed Emami^{a,*}, Mehdi Valipour^{a,b}, Fatemeh Kazemi Komishani^c,
Fatemehsadat Sadati-Ashrafi^c, Maria Rasoulia^d, Majid Ghasemian^e, Mahmood Tajbakhsh^f,
Patrick Honarchian Masihi^d, Aidin Shakiba^d, Hamid Irannejad^a, Nematollah Ahangar^{g,*}

^a Department of Medicinal Chemistry and Pharmaceutical Sciences Research Center, Faculty of Pharmacy, Mazandaran University of Medical Sciences, Sari, Iran

^b Student Research Committee, Faculty of Pharmacy, Mazandaran University of Medical Sciences, Sari, Iran

^c Department of Chemistry, Qaemshahr Branch, Islamic Azad University, Qaemshahr, Iran

^d Student Research Committee, Ramsar Campus, Mazandaran University of Medical Sciences, Ramsar, Iran

^e Department of Clinical Biochemistry, School of Medicine, Shahid Beheshti University of Medical Sciences (SBMU), Tehran, Iran

^f Department of Organic Chemistry, Faculty of Chemistry, University of Mazandaran, Babolsar, Iran

^g Department of Pharmacology, School of Medicine, Guilan University of Medical Sciences, Rasht, Iran

ARTICLE INFO

Keywords:

Anticonvulsant agents
Epilepsy
Hydrazide-hydrazones
MES
PTZ

ABSTRACT

In this study, a series of new isatin aroylhydrazones (**5a-e** and **6a-e**) was synthesized and evaluated for their anticonvulsant activities. The (*Z*)-configuration of compounds was confirmed by ¹H NMR. *In vivo* studies using maximal electroshock (MES) and pentylenetetrazole (PTZ) models of epilepsy in mice revealed that while most of compounds had no effect on chemically-induced seizures at the higher dose of 100 mg/kg but showed significant protection against electrically-induced seizures at the lower dose of 5 mg/kg. Certainly, *N*-methyl analogs **6a** and **6e** were found to be the most effective compounds, displaying 100% protection at the dose of 5 mg/kg. Protein binding and lipophilicity (logP) of the selected compounds (**6a** and **6e**) were also determined experimentally. *In silico* evaluations of title compounds showed acceptable ADME parameters, and drug-likeness properties. Distance mapping and docking of the selected compounds with different targets proposed the possible action of them on VGSCs and GABA_A receptors. The cytotoxicity evaluation of **6a** and **6e** against SH-SY5Y and Hep-G2 cell lines indicated safety profile of compounds on the neuronal and hepatic cells.

1. Introduction

Epilepsy is one of the most common brain disorders that associated with spontaneous seizures followed by neurobiological, cognitive, and psychosocial troubles [1]. Nearly 80% of epileptic patients live in poor countries and over 75% of them are untreated [2]. The causes of epilepsy are related with genetic, structural, metabolic, infectious, immune, and unknown factors [3]. Epileptic seizures such as generalized tonic-clonic happen particularly with loss of consciousness, falls, bilateral rhythmic jerking of nearly all skeletal muscles and marginal or no breathing with cyanosis [4]. Thus these disorders can seriously disrupt the lives of affected patients.

Currently, the long-term use of antiepileptic drugs (AEDs) is the main approach for managing of epilepsy. However, high percentage of patients require poly-therapy to control their seizures [5]. On the other

hand, the use of multiple AEDs increases the risk of drug interactions via enzymatic induction or inhibition, and alterations in protein-binding [6]. These pharmacokinetic interactions may result in low efficacy or high toxicity of AEDs [7]. Thus, the most challenges of AEDs are the high incidence of adverse effects during consumption and major interactions with other medications [8,9]. Due to such problems, conducting new researches to find AEDs with better therapeutic effects seems to be necessary. So far, many efforts have been made to improve therapeutic effects and reducing the toxicity of AEDs.

Accordingly, many newer chemical structures with antiepileptic activity have been identified [10–12]. Isatin (indole-2,3-dione) is an indole-derived chemical structure that identified in human body as a natural metabolite and possesses a broad range of pharmacological and biological activities [13,14]. One of the most important effects of isatin-containing structures is anticonvulsant activity [15–18]. Generally,

* Corresponding authors.

E-mail addresses: semami@mazums.ac.ir (S. Emami), n.ahangar@gums.ac.ir (N. Ahangar).

<https://doi.org/10.1016/j.bioorg.2021.104943>

Received 28 September 2020; Received in revised form 10 February 2021; Accepted 20 April 2021

Available online 24 April 2021

0045-2068/© 2021 Elsevier Inc. All rights reserved.

anticonvulsant structures require functional groups like C=O and N—H as H-bond acceptor and donor which found in isatin [19].

On the other hand, hydrazones are versatile organic compounds usually formed by the reaction of substituted hydrazines and appropriate ketones or aldehydes. Certainly, aroylhydrazones were considered frequently due to their diverse biological properties including anti-mitotic [20], antibacterial [21], anticancer [22], anti-inflammatory [23], anti-hypertensive [24], and anti-platelet [25] activities. In numerous studies, hydrazone group have been used as a main scaffold for the design of new anticonvulsant agents [26–28]. As an example, the hydrazide-hydrazones **A** (Fig. 1) were investigated as anti-seizure agents in the animal model of epilepsy, being effective against maximal electroshock (MES)-induced seizures [27]. Particularly, in some studies both hydrazone and isatin building blocks have been concurrently used to design anticonvulsant agents, as exemplified by compounds **B–D** in Fig. 1 [19,29,30].

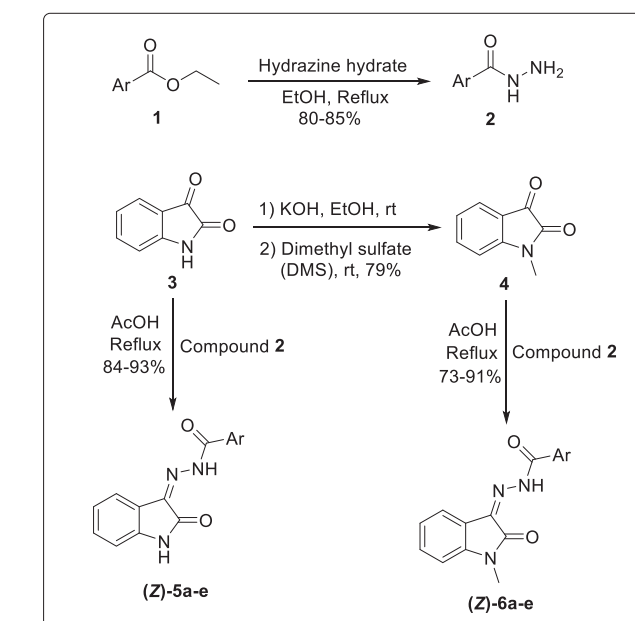
In continuation of our previous work to discovery of hydrazone-containing anticonvulsant agents [26], we have designed compounds **5** and **6**, bearing isatin hydrazone framework. Thus, we report here synthesis, structural characterization, molecular modeling, and *in vitro* and *in vivo* evaluations of *N*-(2-oxoindolin-3-ylidene)benzohydrazides **5** and **6** as new anticonvulsant agents (Fig. 1).

2. Results and discussion

2.1. Chemistry

The title compounds were synthesized according to the route illustrated in Scheme 1. At first, ethyl esters **1** were reacted with hydrazine hydrate in EtOH to give hydrazide derivatives **2**. These compounds also could be prepared from methyl esters as well [31]. On the other hand, 1-methylindoline-2,3-dione (*N*-methyl isatin, **4**) was synthesized by the reaction of isatin (**3**) and dimethyl sulfate in the presence of KOH at room temperature [32].

Thereafter, the condensation of hydrazides **2** with isatin (**3**) or *N*-methyl isatin (**4**) in ethanol in the presence catalytic amount of glacial acetic acid gave the final hydrazide-hydrazone compounds (**5a–e** or **6a–e**).



Scheme 1. Synthesis of isatin-hydrazone derivatives **5a–e** and **6a–e**.

e) [33–35]. The reaction was stirred under reflux for 6 h to complete, monitoring by TLC. The desired product was precipitated after cooling and the resulting precipitate was then filtered and rinsed eventually with cool ethanol, affording high yield.

Generally, the structures of all final compounds were characterized by ^1H NMR, ^{13}C NMR, IR, MS and elemental analyses. Depending on which group is present on the nitrogen of isatin ring, the ^1H NMR spectra of compounds were different. In the spectra of *N*-methyl derivatives (**6a–e**), a singlet signal appears in the region of 3.25 to 3.34 ppm, corresponding to the methyl group. For derivatives without the methyl group (**5a–e**), a singlet signal appears about 11.4 ppm, relating to the NH of isatin. The first signal observed with the least chemical shift in aromatic

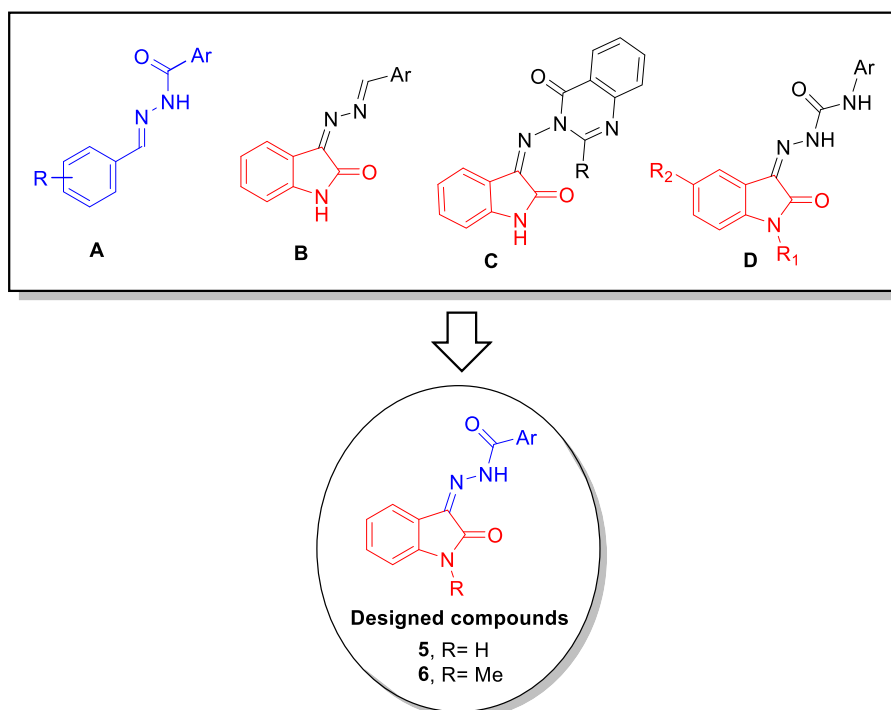


Fig. 1. General structure of our new target compounds **5** and **6** designed based on leads **A–D**.

protons relates to the H-7 of isatin, which appears as a doublet signal in the region of 6.92 to 7.17 ppm ($J = 7.6\text{--}8.0$ Hz). The H-5 of the isatin ring appears as triplet in the range of 7.09 to 7.20 ppm with the coupling constant of 6.8–8.0 Hz. Also, the H-6 of the isatin is observed in the region of 7.36 to 7.48 ppm ($J = 7.2\text{--}8.2$ Hz). The next signal that observed at 7.59 to 7.99 ppm relates to the H-4. The aryl part of the target compounds showed appropriate signals in the range of 6.94 to 8.97 ppm depending on the type of substituent. The last signal observed in the downfield of spectra is related to the NH of hydrazone which appears as a singlet around 14 ppm.

Structurally, our new isatin arylhydrazones (**5a-e** and **6a-e**) can exist in (*E*)- and (*Z*)-isoforms. As shown in Fig. 2, in the chemical structure of the (*Z*)-form, there is the possibility of intramolecular H-bonding between the hydrogen atom of the hydrazone section and the oxygen atom of the adjacent carbonyl group.

Accordingly, we expected that our compounds be in the (*Z*)-geometry. Chemical shift evaluations in the ^1H NMR spectra of compounds **5** and **6** clearly confirm the (*Z*)-conformation. Unlike computational simulations that predict the chemical shifts of NH about 10.87 ppm, but the observed chemical shifts were in the range of 13.89 to 14.23 ppm (Table 1). The emergence of NH signal in this area confirms the existence of intramolecular hydrogen bonding in the (*Z*)-form [36,37].

2.2. In vivo studies

Experimental animal models of epilepsy represent different type of human epilepsies. The maximal electroshock (MES)-induced seizure is a mechanism-independent model of epilepsy which often used for screening of anticonvulsant agents. This test represents the human grand mal form of epilepsy [38]. Pentylentetrazole (PTZ) is a GABA_A receptor antagonist that can be used to induce seizures in rodents. In processes related to the discovery of new antiepileptic drugs, PTZ test is one of the most widely used animal model for evaluating the effects of novel compounds. This model simulates petit mal or absence seizures in humans [39].

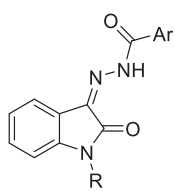
In this study, the anticonvulsant activity of novel derivatives **5a-e** and **6a-e** was evaluated by using MES and PTZ models in mice.

2.2.1. MES test

The final compounds **5a-e** and **6a-e** were administered intraperitoneally (i.p.) to mice at the doses of 5, 10 and 30 mg/kg bw, 30 min before the induction of seizure by electroshock. The number of mice protected against MES-induced convulsions was recorded 30 min after treatment (Table 2). The obtained results showed that most of the new compounds were effective in the MES model even at the dose of 5 mg/kg. Among the tested compounds, the *N*-methylisatin analogs **6a** and **6e** showed 100% protection against electrically-induced seizures at the dose of 5 and 10 mg/kg. Furthermore, unsubstituted compound **5a** showed 100% protection at the lower dose of 5 mg/kg. In the *N*-desmethyl series, 4-tolyl and 4-nitrophenyl analogs (**5c** and **5e**, respectively) showed full protection at the dose of 10 mg/kg. The maximum protection of 75% was

Table 1

Experimental ^1H NMR chemical shifts (ppm) of NN-H proton of (*Z*)-isoforms versus predicted theoretical chemical shifts in the title compounds.



Compounds	R	Ar	Experimental chemical shift	Theoretical chemical shift ^a
5a	H	Phenyl	13.96	10.87
5b	H	4-Hydroxyphenyl	13.88	10.87
5c	H	4-Methylphenyl	13.91	10.87
5d	H	4-Chlorophenyl	13.89	10.87
5e	H	4-Nitrophenyl	14.00	10.87
6a	CH ₃	Phenyl	14.11	10.87
6b	CH ₃	4-Hydroxyphenyl	14.23	10.87
6c	CH ₃	4-Methylphenyl	13.83	10.87
6d	CH ₃	4-Chlorophenyl	14.06	10.87
6e	CH ₃	4-Pyridinyl	14.12	10.87

^a Theoretical chemical shift, predict by ChemDraw professional (CambridgeSoft, Billerica, MA, USA).

observed for the less potent compounds **5b**, and **6b-6d** at the higher dose tested (30 mg/kg).

As seen from MES data, the simplest compound with no substituent on the aryl part (compound **5a**) showed high potency. Introduction of 4-hydroxy on the benzoyl hydrazone resulted in compound **5b** with less activity, indicating that the OH group diminishes the anti-MES activity. By comparison of compounds **5a** and **5b** with the *N*-methyl counterparts **6a** and **6b**, it can be concluded that the *N*-methylation of isatin nucleus increases the protective activity against MES-induced convulsions. Surprisingly, the insertion of chloro substituent on the *para*-position of benzoyl moiety had negative effect on the anticonvulsant activity (compare **5d** with **5a**, or **6d** with **6a**). However, the electron withdrawing group NO₂ could be tolerated with reserving the activity. Replacement of phenyl with 4-pyridinyl in compound **6a** resulted in highly potent compound **6e**.

2.2.2. PTZ test

In addition to MES, all the synthesized compounds were investigated for their anti-seizure potential against PTZ-induced convulsions and mortality in mice. All the compounds were administered intraperitoneally (i.p.), 30 min before the injection of PTZ (100 mg/kg). The number of animals protected against PTZ-induced seizures was recorded 30 min after treatment. As listed in Table 2, most of compounds had no effect on the PTZ-induced seizures at the doses of 30 or 100 mg/kg. Compounds **5c** and **6a** could protect only 25% of mice against PTZ. Notably, previous animal studies on the marketed anticonvulsants revealed that many of them are only effective on some experimental animal models. For example, phenytoin that is one of the most well-known antiepileptic drugs, has been shown to be effective in modifying experimental seizures induced by MES, but failed to antagonize clonic seizures induced by PTZ and strychnine [40].

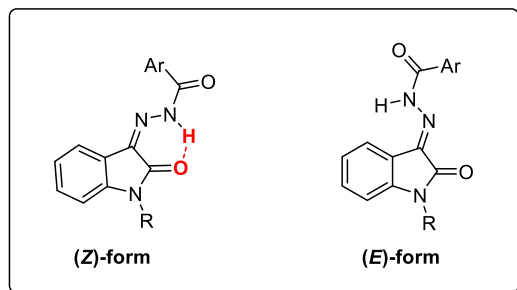


Fig. 2. Possible geometry of title compounds **5** and **6**, and presentation of potential intramolecular H-bond in the (*Z*)-form.

Table 2Anticonvulsant screening results of test compounds **5a-e** and **6a-e**.

	MES ^a						PTZ ^b			
Compounds	5mg/kg	Protection (%)	10mg/kg	Protection (%)	30mg/kg	Protection (%)	30mg/kg	Protection (%)	100 mg/kg	Protection (%)
5a	4/4	100	3/4	75	3/4	75	–	–	0/4	0
5b	1/4	25	2/4	50	3/4	75	–	–	0/4	0
5c	3/4	75	4/4	100	–	–	0/4	0	1/4	25
5d	2/4	50	3/4	75	1/4	25	–	–	0/4	0
5e	2/4	50	4/4	100	–	–	–	–	0/4	0
6a	4/4	100	4/4	100	–	–	0/4	0	1/4	25
6b	3/4	75	3/4	75	3/4	75	–	–	0/4	0
6c	– ^c	–	1/4	25	3/4	75	–	–	0/4	0
6d	0/4	0	1/4	25	3/4	75	–	–	0/4	0
6e	4/4	100	4/4	100	–	–	–	–	0/4	0
Diazepam ^d	4/4	100	–	–	–	–	–	–	4/4	100
Vehicle	0/4	0	–	–	–	–	–	–	0/4	0

^a Maximal electroshock (number of mice protected/number of mice tested)^b Pentylenetetrazole (i.p.) (number of mice protected/number of mice tested)^c Not tested.^d Diazepam was tested at the dose of 2 mg/kg.

2.2.3. *In vivo* neurotoxicity of promising compound **6e**

The rotarod test is utilized extensively to evaluate motor coordination and neurotoxic effects of new molecules in rodents. In this regard, the potential of compound **6e** for neurological impairment was evaluated by the measurement of ability to maintain balance on a rotating rod for long periods of time. Result of this test was presented in Table 3. Unlike diazepam, compound **6e** was well tolerated at different times (0.5, 1, 2 and 4 h after treatment) and all treated-mice were able to maintain their balance on the rotating rod for at least 30 s. These results indicated that the representative compound **6e** has less effect on the motor coordination respect to the standard drug diazepam.

2.3. *In vitro* studies

2.3.1. Cell viability assay

In order to check the safety profile of our compounds, the most effective anti-seizure compounds (**6a** and **6e**) on MES were subjected to cytotoxicity evaluation on SH-SY5Y and HepG2 cell lines, using MTT colorimetric assay. As presented in Fig. 3, both compounds exhibited significant cytotoxic effect only at concentrations equal or higher than 160 µg/ml. The determined IC₅₀ values of compound **6a** against HepG2 and SH-SY5Y were 805.9 and 822.1 µM, respectively. Based on data shown in Fig. 3, the IC₅₀ values of **6e** were estimated to be 786.7 and 693.2 µM toward HepG2 and SH-SY5Y cells, respectively. These findings revealed that the selected compounds at conventional concentrations had no effect on HepG2 and SH-SY5Y, as *in vitro* models of hepatic and neuronal cells.

2.3.2. Plasma protein binding (PPB) determination

Human serum albumin (HSA) is the main protein in the blood plasma and plays as a transport protein in the body. Frequently, CNS active drugs such as anti-epileptics have a high affinity for plasma proteins and bind to HSA in a reversible process. The PPB of CNS active drugs has a significant impact on their activity because only the free unbound drug is just available to pass through the BBB. Actually, PPB controls the free drug concentrations in plasma. However, there are also some anti-epileptic drugs owning high levels of protein binding (i.e., > 90%), including phenytoin, valproic acid, tiagabine, and perampanel [41]. Also, there is a high correlation between lipophilicity and the degree of PPB of drugs, but lipophilicity is not the sole determinant [42]. Accordingly, in this study, we attempted to evaluate the extent of the binding profile of the new compounds **6a** and **6e** to the plasma albumin protein using experimental and computational methods. To this end, we measured the PPB rate of compounds **6a** and **6e** at concentrations similar to those of standard drugs in the body [43]. Since bovine serum albumin (BSA) and HSA are homologous proteins and their interactions

Table 3Assessment of the motor coordination and skeletal muscle relaxant effects of compound **6e** on mice, using rotarod test.

Compounds	Dose (mg/kg)	Animals	0.5 h	1 h	2 h	4 h
6e	2.5	1	> 60 ^a	> 60	> 60	> 60
		2	> 60	> 60	> 60	> 60
		3	> 60	> 60	> 60	> 60
		4	> 60	> 60	> 60	> 60
	5	1	> 60	> 60	> 60	> 60
		2	> 60	> 60	> 60	> 60
		3	54.81 ± 5.64	> 60	> 60	> 60
		4	> 60	> 60	> 60	> 60
	10	1	> 60	> 60	> 60	> 60
		2	30.67 ± 2.85	> 60	> 60	> 60
		3	44.12 ± 7.13	> 60	> 60	> 60
		4	> 60	> 60	> 60	> 60
	Vehicle	1	> 60	> 60	> 60	> 60
		2	> 60	> 60	> 60	> 60
		3	> 60	> 60	> 60	> 60
		4	> 60	> 60	> 60	> 60
Diazepam	2	1	0	4.7 ± 0.61	41.3 ± 6.95	> 60
		2	0	6.6 ± 1.91	29.6 ± 4.63	> 60
		3	0	13.3 ± 2.63	> 60	> 60
		4	0	8.7 ± 3.13	> 60	> 60

^a The measurement was repeated three times for each trial, and the results were presented as average. For mice that were able to maintain their balance on the rotating rod for >60 s, the measurement was not repeated.

with drugs have been extensively studied, we used BSA at a concentration of 40 mg/ml (the normal concentration of HSA in the blood serum is 35–50 mg/ml) [33,44]. High performance liquid

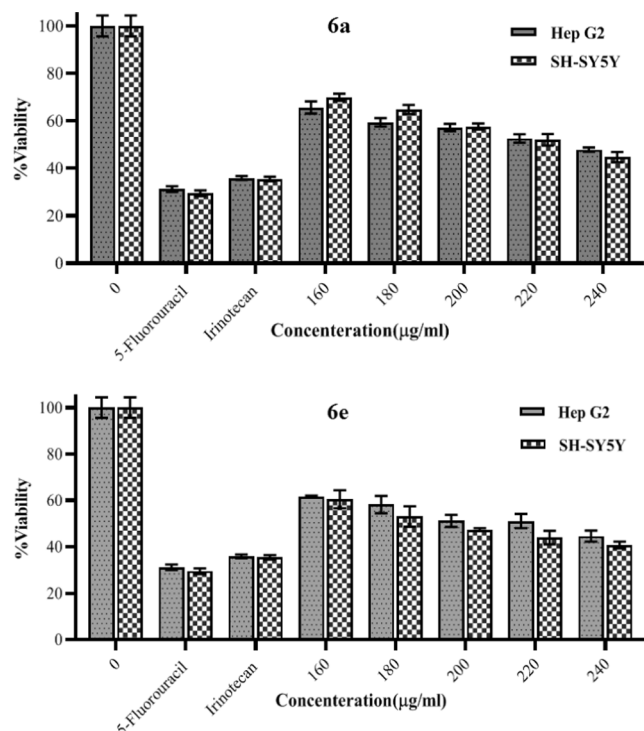


Fig. 3. Effects of compounds **6a** and **6e** at different concentrations on the viability of HepG2 and SH-SY5Y cell lines in comparison with reference drugs Irinotecan and 5-Fluorouracil (at the concentration of 40 µg/ml).

chromatography (HPLC) method was used to measure plasma protein binding, experimentally. Furthermore, PreADME online server was used to predict plasma protein binding computationally. The obtained results from both methods are shown in Table 4. The PPB rate for **6a** was higher than that of **6e** in both computational and experimental methods. This difference could be due to the more lipophilic character of phenyl ring in the compound **6a** compared to the pyridin-4-yl in the counterpart compound **6e**.

2.3.3. Measurement of Log *p* (Lipophilicity)

In this study, we measured the 1-octanol/water partition coefficient (Log *P*) of the promising compounds **6a** and **6e** by using of HPLC method (Table 5). Also, SwissADME online server was used to predict Log *P*. Comparison of the experimental and computational values of Log *P* indicates that the value of Log *P* calculated by the experimental method is significantly higher than value calculated by computational method. As described above, the title compounds form intramolecular hydrogen bond, and their predominant structure is (*Z*)-configuration. This situation may lead to higher lipophilicity of the compounds respect to the computationally calculated value [45].

2.4. In silico studies

Nowadays, *in silico* studies have become a critical filter in drug discovery process. In this study, all the compounds were subjected to the prediction of toxicity, ADME properties and drug-likeness parameters.

Table 4
Estimated plasma protein binding (PPB) rate (%) of the compounds **6a** and **6e**.

Method	6a	6e
Computational	96.23	85.01
Experimental ^a	~100	74.96 ± 3.25

^a Bovine serum albumin (BSA) was used to evaluate the PPB of the tested compounds.

Table 5

Experimental and computational Log *P* of the selected compounds.

Log <i>P</i>	6a	6e
Computational Log <i>P</i> _{o/w} (iLOGP)	2.27	1.88
Computational Log <i>P</i> _{o/w} (XLOGP3)	2.90	1.83
Computational Log <i>P</i> _{o/w} (SILICOS-IT)	2.27	1.72
Experimental Log <i>P</i> _{o/w}	3.58 ± 0.21	3.16 ± 0.25

Since our compounds are designed as anticonvulsants, computational CNS-bioavailability of them was predicted by assessment of physico-chemical descriptors such as MW (molecular weight), log*P*, TPSA (topological polar surface area), number of rotatable bonds, and hydrogen bond donors/acceptors counts in the molecules. All these parameters were calculated using SwissADME and PreADME online servers.

2.4.1. Drug-likeness parameters

Lipinski's rule of five (RO5) is a general rule for evaluating the drug-likeness of chemical compounds that having specific pharmacological or biological activity. According to RO5, good absorption and permeability can be achieved when the molecule has the following characteristics: MW ≤ 500, Log *P* ≤ 5, Hydrogen bond donors ≤ 5, Hydrogen bond acceptor ≤ 10, and number of rotatable bonds ≤ 10. Lipinski also laid down a set of rules for good CNS penetration. According to these rules, good CNS penetration can be achieved when: MW is ≤ 400, Log *P* ≤ 5, Hydrogen bond donor ≤ 3 and Hydrogen bond acceptor ≤ 7 [46]. Given the importance of Lipinski's rules in expressing the drug-likeness of new compounds, we examine here each of these parameters in detail for our compounds.

Molecular weight: In general, CNS active agents have significantly reduced MW compared to other therapeutics. Some previous studies also suggested that MW should be kept below 450 to facilitate brain penetration [47]. Previously, in a study that conducted by Leeson and Davis, the mean MW value for marketed CNS drugs was reported to be <310 g/mol [48]. According to the results that presented in Table 6, calculated MW for our compounds is in the range of 265 to 314 g/mol, which can be ideal for activity in CNS.

Log*P* (Lipophilicity): The lipophilicity is one of the most important descriptors for the penetration of compounds into the CNS. According to computational predictions, some of our compounds were found to be lipophilic enough (Log*P* > 2) and have appropriate potential to cross the blood brain barrier (BBB). However, for some others, this parameter is lower (Log *P* < 2). These results may initially indicate that these derivatives have difficulty to cross the BBB, because of low lipophilicity. But the remarkable issue about the structure of these compounds is the ability to form intramolecular hydrogen bonds (Fig. 2). The formation of intramolecular H-bonds in chemical structure of drugs is hypothesized to shield polarity, improving the membrane permeability. Some studies have confirmed the key role of intramolecular hydrogen bonding in enhancing BBB penetration [49].

Number of hydrogen bond donor/acceptor: The ability of a molecule in creating hydrogen bonds can be detected by hydrogen bond donors (N–H and O–H) and acceptors (N, O and F) counts. In general, molecules with high H-bonding potential have minimal BBB permeability. Leeson et al. showed that the marketed CNS drugs have (O + N) = 4.32, PSA = 16.3%, H-bond acceptors = 2.12 and H-bond donors = 1.5, averagely [48]. As shown in Table 6, the number of H-bond donor atoms for all of our compounds is in the range of 1 to 3, and the number of H-bond acceptors is in the range of 3 to 5, that all results are in the appropriate range for CNS-active compounds.

Number of rotatable bonds: The number of rotatable bonds is another descriptor that widely used as a filter in drug discovery. Molecular flexibility is actually related to rotatable bonds and the number of rings in the structure of molecule. This descriptor determines the accessible conformations in the molecule under different physiological conditions. Results of bioavailability studies showed that >10 rotatable bonds

Table 6Drug-like properties of compounds **5a-e** and **6a-e**, calculated using SwissADME and PreADME online servers.

Parameters	5a	5b	5c	5d	5e	6a	6b	6c	6d	6e
MW ^a	265.27	281.27	279.29	299.71	310.26	279.29	295.29	293.32	313.74	280.28
Log P ^b	1.92	1.38	2.13	2.33	1.26	2.15	1.66	2.35	2.54	1.41
nRB ^c	3	3	3	3	4	3	3	3	3	3
nHBA ^d	3	4	3	3	5	3	4	3	3	4
nHBD ^e	2	3	2	2	2	1	2	1	1	1
Lipinski V ^f	0	0	0	0	0	0	0	0	0	0
PPB ^g	91.50	79.66	92.27	90.72	79.57	96.23	85.64	96.35	94.88	85.01
TPSA ^h	70.56	90.79	70.56	70.56	116.38	61.77	82.00	61.77	61.77	74.66

^a Molecular weight.^b Log P octanol/water partition coefficient, average of five prediction Log Po/w (iLOGP), Log Po/w (XLOGP3), Log Po/w (WLOGP), Log Po/w (MLOGP), Log Po/w (SILICOS-IT).^c Number of rotatable bonds.^d Number of H-bond acceptors.^e Number of H-bond donors.^f Violations of Lipinski rule of 5 (logP < 5, MW < 500, nHBA < 10, and nHBD < 5).^g In vitro plasma protein binding (%).^h Topological polar surface area.

correlate with decreasing in oral bioavailability [50]. Generally, CNS-active drugs contain fewer rotatable bonds (five or less) compared to other drugs [48]. Based on the results presented in Table 6, the number of rotatable bonds for all of our compounds is in the range of 3 to 4, which can be ideal for CNS active agents.

In general, these results demonstrate that all synthesized compounds have no violation of Lipinski rule of 5 and are completely drug-like compounds. Thus, it expected that the prototype compounds have suitable oral bioavailability.

2.4.2. In silico prediction of cytochrome P450 interactions

Hepatotoxicity is one of the main problems of many antiepileptic drugs, such as valproic acid, phenytoin, and felbamate [51]. Cytochrome P450 enzymes play an important role in the pharmacological and toxicological effects of drugs. The most famous isoforms of these enzymes that are vital in the metabolism of drugs are CYP3A4, CYP2D6, CYP2C9, and CYP2C19. Successful antiepileptic drugs with maximum oral absorption must have no significant CYP2D6 metabolism and be non-potent CYP3A4 inducers. Also, compounds that are potent inhibitors of CYP3A4 and CYP2D6 enzymes, have a high chance for inhibiting the metabolism of co-administered drugs [52]. Because of the importance of drug interactions with Cytochrome P450 enzymes, we tried to predict the inhibitory effects of the title compounds on these enzymes by using PreADME and SwissADME online servers. The results of the evaluations are shown in Table 7. According to these results, it can be expected that most of the synthesized compounds had no effects on the CYP3A4, CYP2D6, CYP2C9 and CYP2C19 enzymes. Notably, it is expected that the more promising anticonvulsant compound **6e** has no effect on the important cytochrome P450 enzymes, displaying minimum interactions with other drugs.

Table 7

Prediction of the inhibitory effects of title compounds on Cytochrome P450 enzymes.

Compounds	CYP2C19 inhibitor	CYP2C9 inhibitor	CYP2D6 inhibitor	CYP3A4 inhibitor
5a	No	No	No	No
5b	No	No	No	No
5c	No	No	No	No
5d	No	No	No	No
5e	No	No	No	No
6a	Yes	Yes	No	No
6b	No	No	No	No
6c	Yes	Yes	No	No
6d	Yes	Yes	No	No
6e	No	No	No	No

2.4.3. Docking study

Molecular docking is the most common method in structure-based drug design studies that has been widely used in drug discovery [53]. AutoDock Vina is a novel and worthy program for molecular docking and virtual screening that significantly can improve the accuracy of the binding mode predictions [54]. Thus, we used this method to investigate the interaction of synthesized compounds with famous molecular targets of antiepileptic agents, VGSCs, GABA_A, NMDA, AMPA and GABA-T. Among the evaluated compounds in animal models, compound **6a** and **6e** were selected for docking, because these compounds showed higher potency in anticonvulsant evaluations. In docking evaluations, diazepam and phenytoin that act through the GABA_A and VGSC receptors were used as references for comparisons [55]. Docking evaluations with mentioned targets were done according to the procedure described in the Experimental section. Although our spectroscopic data showed that the title compounds have (Z)-configuration, but the isomerization of hydrozone is also possible due to the rotation and inversion of C=N double bond [56]. Therefore, we investigated docking of both (E and Z)-isomers of **6a** and **6e**.

The lowest free energies obtained from the binding of (E/Z)-isomers of **6a** and **6e** and standard drugs are summarized in Table 8. Diazepam has the lowest free energy of binding for GABA_A receptor with ΔG of −10.20 kcal/mol. As shown in Table 8, binding free energy of both (E)- and (Z)-isomers of **6a** and **6e** to the VGSCs and GABA_A receptors was the lowest ΔG among the tested targets.

The amount of binding free energy of both (E)- and (Z)-isomers of **6a** and **6e** are not much different. These compounds exhibit quite similar interactions at the active site of the VGSCs. As seen in Fig. 4, the carbonyl group of the hydrazide moiety in both compounds forms a hydrogen bond with Arg1602. Furthermore, pi-alkyl, alkyl and amide-pi-stacked interactions are observed between Arg1605, Arg1602 and Ala1604 with the phenyl or pyridinyl moiety of **6a** and **6e**, respectively. The isatin moiety in both compounds has alkyl and pi-alkyl interactions with Ala1585, Val1541 and Tyr1537. Furthermore, pi-cation interactions are observed between Tyr1537 and one of the middle

Table 8Binding free energy (in kcal/mol) of phenytoin, diazepam and (E/Z) isomers of **6a** and **6e** on five targets.

Compounds	VGSCs	GABA _A	GABA-T	NMDA	AMPA
Phenytoin	−9.70	−9.70	−8.00	−8.40	−8.10
Diazepam	−9.10	−10.20	−7.70	−8.20	−8.30
(E)- 6a	−10.0	−9.90	−8.20	−9.40	−8.00
(Z)- 6a	−9.90	−9.80	−8.00	−9.00	−8.40
(E)- 6e	−9.90	−9.60	−7.60	−8.50	−9.30
(Z)- 6e	−9.60	−9.50	−7.60	−8.50	−9.30

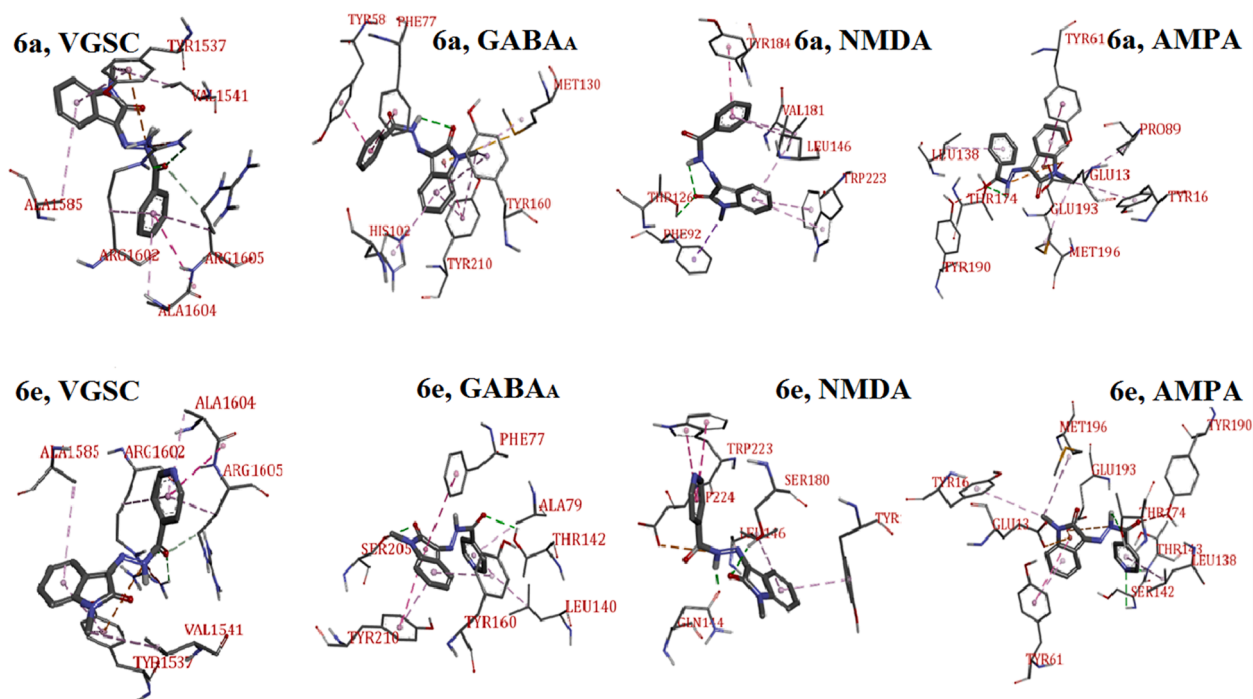


Fig. 4. 3D interactions of compounds **6a** and **6e** in the active site of VGSCs, GABA_A, AMPA, and NMDA and GABA-T targets.

nitrogens in both compounds **6a** and **6e**. Rest of the interactions between compounds **6a** and **6e** with the other targets are shown in Fig. 4. Representatively, the most important interactions of the compound **6e** are shown in two-dimensional (2D) form in Fig. 5.

The docking results suggested that the binding with VGSCs and GABA_A receptor is the most possible mechanism of action for these compounds. However, based on the animal studies, our compounds has been shown to be effective in modifying experimental seizures induced by MES, but failed to antagonize convulsions induced by PTZ. Some studies indicated that false negative results might be observed in both PTZ and MES rodent models. For example, phenytoin and carbamazepine, as well-known VGSC inhibitors showed no efficacy in PTZ model while exhibiting good efficacy in the MES model. Moreover, there are fewer drugs such as vigabatrin with negative results in the MES model

which could be effective in the PTZ model [57]. In addition, there are several factors could influence anticonvulsant potency in the PTZ model: i) bi-shaped dose–response curve i.e., a decline in anticonvulsant response at high doses of some compounds, leading to misinterpretation of drug efficacy if only a single high drug dose is experimented; ii) effects of route of PTZ administration (i.v. infusion, s.c. or i.p. injection) on estimation of anticonvulsant potency; and iii) species differences in drug metabolism [58]. Therefore, despite the possible tendency of the tested compounds to VGSC and/or GABA receptors, the above mentioned factors might be involved in our experiments resulting in the lack of activity in the PTZ model.

2.4.4. Distance mapping

Previously, the essential pharmacophoric features which could be

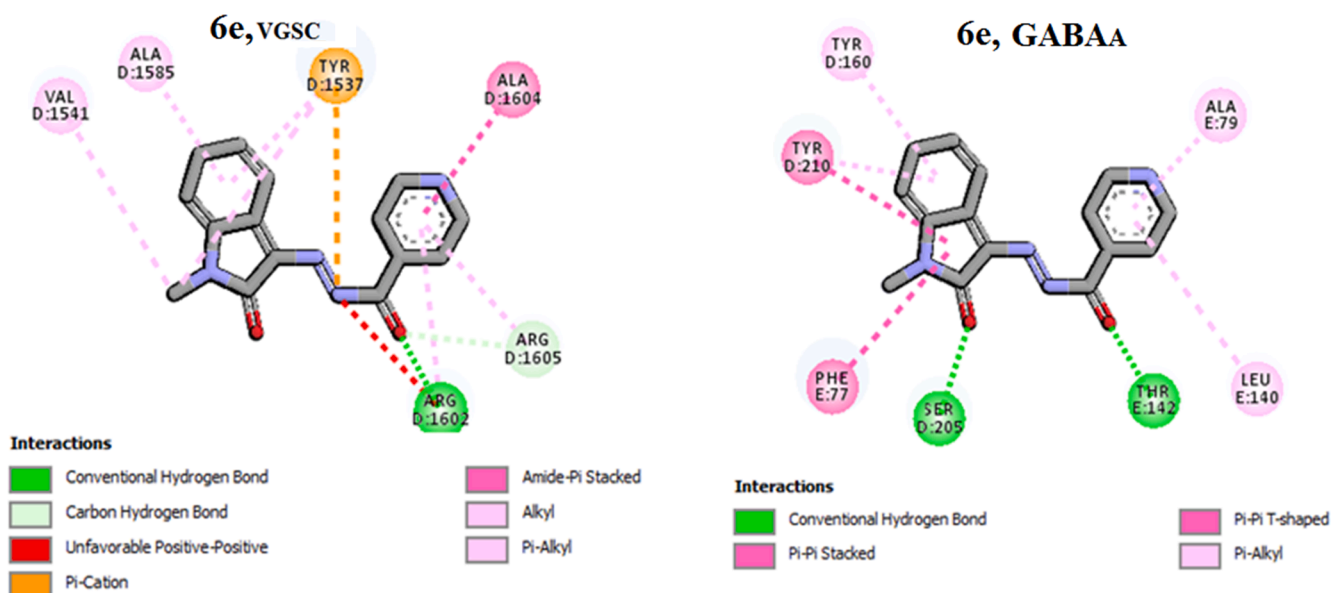
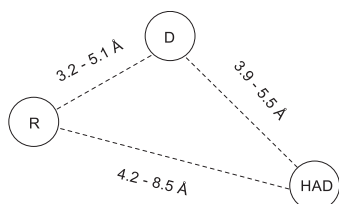


Fig. 5. 2D presentation for interaction mode of compound (Z)-**6e** in the active site of VGSCs and GABA_A.

Table 9

Distances of pharmacophoric points of the selected compounds **6a** and **6e** and some conventional antiepileptic drugs based on the suggested pharmacophore model for acting on the VGSCs.



Compound	R-D (Å)	R-HBD (Å)	D-HBD (Å)
Carbamazepine	4.2	5.4	4.7
Phenytoin	3.3	4.7	3.3
Nafimidone	4.3	4.9	4.5
(E)- 6a	3.5	4.9	5.6
(Z)- 6a	3.5	5.0	4.8
(E)- 6e	3.5	4.9	5.3
(Z)- 6e	3.5	5.1	4.8

R: Hydrophobic unit; D: Electron donor; HBD: Hydrogen bonding domain; Distances in Angstrom (Å) were measured after geometry optimization of compounds in Molegro molecular viewer.

necessary for interacting with the active site of VGSCs have been established by Unverferth et al. as a distance mapping model [59]. The calculated distance ranges between the pharmacophoric elements of anticonvulsants acting on the VGSCs are shown in Table 9. Accordingly, we measured the distances between these pharmacophoric parts in the structure of our compounds. The measured distances are summarized in Table 9. In our distance mapping evaluations, carbamazepine, phenytoin, and nafimidone that have anticonvulsant effects by the blocking of VGSCs mechanism, have been used as standard drugs. As shown in Table 9, all distances between the pharmacophoric points R-D, D-HBD and R-HBD of our compounds have been in the ranges measured for standard anticonvulsant drugs. Based on this modeling, blockage of VGSCs could be one of the possible mechanisms of our compounds in suppressing seizures.

3. Conclusion

We have synthesized a number of isatin aroylhydrazones and characterized their structures as (Z)-isomer. The *in vivo* tests indicated that most of them are effective against MES-induced seizures in mice even at the low dose of 5 mg/kg. In particular, the *N*-methylisatin derivatives **6a** and **6e** can fully protect mice (100% protection) against electrically-induced seizures at the dose of 5 mg/kg. The *in silico* evaluations showed that these compounds have good drug-like properties as CNS-active agents. The docking study of the promising compounds **6a** and **6e** with different targets suggested that the binding with VGSCs and GABA_A receptor is the most possible mechanism of action for these compounds. The *in vitro* cytotoxicity assay revealed that the selected compounds at conventional concentrations had no effect on HepG2 and SH-SY5Y cell lines.

4. Experimental

4.1. Chemistry

All the starting materials, solvents, and reagents required in this study were purchased from Sigma-Aldrich and Merck suppliers. The Silica Gel 60 F254 TLC Plastic Sheets (Merck, AG Darmstadt, Germany) were used for thin-layer chromatography of samples.

4.1.1. General procedure for the synthesis of arylhydrazides 2

The intermediate hydrazides **2** were prepared from appropriate

esters **1** according to the reported method [31]. Briefly, to a solution of ethyl ester (**1** mmol) in EtOH, hydrazine hydrate (128 mg, 4 mmol) was added and the mixture was refluxed overnight. After evaporation of the solvent under reduced pressure, the residue was poured into ice. The precipitate was separated by filtration and washed with cold EtOH to give desired hydrazide compound.

4.1.2. Synthesis of *N*-methylisatin (4)

To a solution of isatin (**3**, 735 mg, 5 mmol) in ethanol (10 ml), potassium hydroxide solution (5 ml) was added and stirred at room temperature for 0.5 h. Then, dimethyl sulfate (0.75 ml) was added and stirring was continued for another 1 h. At the end (monitored by TLC), the reaction mixture was filtered to remove salts. After concentrating the solution, water was added to the residue and placed in the refrigerator. The resulting solid was separated and washed with water to obtain the desired *N*-methyl product **4**.

4.1.3. General procedure for the synthesis of isatin aroylhydrazones (5a-e and 6a-e)

To a solution of isatin (**3**, 147 mg, 1 mmol) or *N*-methyl isatin (**4**, 161 mg, 1 mmol) in ethanol (4–5 ml), arylhydrazides **2** (1 mmol) and a drop of glacial acetic acid was added. The reaction mixture was stirred under reflux for 6 h, and progress the reactions were monitored by TLC. After consuming the starting materials, the reaction was cold to room temperature and placed in the refrigerator overnight to complete deposition. Then, the precipitated solid was filtered off and washed with ethanol to yield final compounds (**5** and **6**) as yellow to orange powder.

(Z)-*N*'-(2-oxoindolin-3-ylidene)benzohydrazide (**5a**). Orange solid; Yield 90%; m.p.: 292–294 °C; IR (KBr, cm⁻¹): 3437, 3233, 3108, 2956, 1693, 1533, 1092; ¹H NMR (400 MHz, CDCl₃) δ: 6.94 (d, 1H, *J* = 8.0 Hz, H-7), 7.17 (dt, 1H, *J* = 8.0 and 0.8 Hz, H-5), 7.38 (dt, 1H, *J* = 8.0 and 1.2 Hz, H-6), 7.55 (t, 2H, *J* = 7.2 Hz, H-3' and H-5'), 7.64 (tt, 1H, *J* = 7.2 and 1.6 Hz, H-4'), 7.83 (br s, 1H, NH Isatin), 7.88 (d, 1H, *J* = 6.8 Hz, H-4), 8.03 (d, 2H, *J* = 7.2 Hz, H-2' and H-6'), 13.96 (s, 1H, NH Hydrazone). ¹³C NMR (100 MHz, DMSO-*d*₆): 111.70, 120.27, 121.45, 123.24, 127.87, 129.65, 132.29, 132.52, 133.35, 138.69, 142.93, 163.53. MS (*m/z*, %): 265 (M⁺, 6), 257 (28), 211 (16), 201 (12), 183 (83), 155 (23), 126 (42), 111 (20), 98 (35), 85 (46), 69 (70), 57 (97), 43 (100). Anal. Calcd for C₁₅H₁₁N₃O₂: C, 67.92; H, 4.18; N, 15.84. Found: C, 67.99; H, 3.97; N, 15.80.

(Z)-4-hydroxy-*N*'-(2-oxoindolin-3-ylidene)benzohydrazide (**5b**). Yellow solid; Yield: 89%; m.p.: 299–301 °C; IR (KBr, cm⁻¹): 3436, 3187, 3119, 2944, 1691, 1538, 1180, 1089; ¹H NMR (400 MHz, DMSO-*d*₆) δ: 6.94 (d, 2H, *J* = 8.8 Hz, H-3' and H-5'), 6.95 (d, 1H, *J* = 7.6 Hz, H-7), 7.10 (dt, 1H, *J* = 7.6 and 0.8 Hz, H-5), 7.38 (dt, 1H, *J* = 7.6 and 1.2 Hz, H-6), 7.59 (d, 1H, *J* = 7.2 Hz, H-4), 7.78 (d, 2H, *J* = 8.8 Hz, H-2' and H-6'), 10.44 (br s, 1H, OH), 11.36 (br s, 1H, NH Isatin), 13.87 (br s, 1H, NH Hydrazone). ¹³C NMR (100 MHz, DMSO-*d*₆): 111.64, 116.26, 120.43, 121.25, 122.89, 123.17, 130.13, 131.21, 131.97, 137.73, 142.69, 162.21, 163.57. MS (*m/z*, %): 281 (M⁺, 1), 257 (24), 211 (15), 183 (78), 155 (14), 127 (28), 111 (17), 98 (34), 85 (38), 71 (48), 57 (100). Anal. Calcd for C₁₅H₁₁N₃O₃: C, 64.05; H, 3.94; N, 14.94. Found: C, 64.18; H, 3.91; N, 14.99.

(Z)-4-methyl-*N*'-(2-oxoindolin-3-ylidene)benzohydrazide (**5c**). Yellow solid; Yield: 84%; m.p.: 297–298 °C; IR (KBr, cm⁻¹): 3436, 3214, 3114, 2935, 1706, 1549, 1089; ¹H NMR (400 MHz, DMSO-*d*₆) δ: 2.39 (s, 3H, CH₃), 6.96 (d, 1H, *J* = 7.6 Hz, H-7), 7.11 (t, 1H, *J* = 7.2 Hz, H-5), 7.36 (dt, 1H, *J* = 7.6 and 1.2 Hz, H-6), 7.40 (d, 2H, *J* = 8.0 Hz, H-3' and H-5'), 7.60 (d, 1H, *J* = 7.6 Hz, H-4), 7.78 (d, 2H, *J* = 8.0 Hz, H-2' and H-6'), 11.42 (br s, 1H, NH Isatin), 13.91 (br s, 1H, NH Hydrazone). ¹³C NMR (100 MHz, DMSO-*d*₆): 21.58, 111.66, 120.31, 121.37, 123.19, 127.87, 129.65, 130.15, 132.16, 138.36, 142.85, 143.68, 163.52. MS (*m/z*, %): 279 (M⁺, 15), 251 (29), 211 (7), 183 (32), 159 (28), 119 (100), 91 (91), 71 (44), 57 (57). Anal. Calcd for C₁₆H₁₃N₃O₂: C, 68.81; H, 4.69; N, 15.05. Found: C, 68.80; H, 4.76; N, 14.92.

(Z)-4-chloro-*N*'-(2-oxoindolin-3-ylidene)benzohydrazide (**5d**). Yellow

solid; Yield: 84%; m.p.: 319–321 °C; IR (KBr, cm^{-1}): 3458, 3220, 3123, 2942, 1719, 1594, 1087; ^1H NMR (400 MHz, $\text{DMSO}-d_6$) δ : 6.95 (d, 1H, $J = 7.6$ Hz, H-7), 7.11 (t, 1H, $J = 7.6$ Hz, H-5), 7.40 (dt, 1H, $J = 7.6$ and 1.2 Hz, H-6), 7.59 (d, 1H, $J = 7.6$ Hz, H-4), 7.69 (d, 2H, $J = 8.4$ Hz, H-3' and H-5'), 7.90 (d, 2H, $J = 8.4$ Hz, H-2' and H-6'), 11.42 (br s, 1H, NH Isatin), 13.89 (br s, 1H, NH Hydrazone). ^{13}C NMR (100 MHz, $\text{DMSO}-d_6$): 111.72, 120.18, 121.50, 123.25, 129.74, 131.28, 132.38, 138.16, 142.99, 163.48. MS (m/z , %): 299 (M^+ , 22), 271 (13), 257 (25), 211 (17), 183 (75), 160 (85), 139 (100), 111 (81), 98 (41), 85 (47), 71 (57), 57 (98). Anal. Calcd for $\text{C}_{15}\text{H}_{10}\text{ClN}_3\text{O}_2$: C, 60.11; H, 3.36; N, 14.02. Found: C, 60.23; H, 3.37; N, 14.09.

(Z)-4-nitro-N'-(2-oxoindolin-3-ylidene)benzohydrazide (**5e**). Orange solid; Yield: 93%; m.p.: 339–341 °C; IR (KBr, cm^{-1}): 3432, 3232, 3113, 2946, 1737, 1598, 1521, 1342, 1143; ^1H NMR (400 MHz, $\text{DMSO}-d_6$) δ : 6.92 (d, 1H, $J = 8.0$ Hz, H-7), 7.09 (t, 1H, $J = 7.6$ Hz, H-5), 7.42 (dt, 1H, $J = 7.6$ and 2.0 Hz, H-6), 7.99 (d, 1H, $J = 7.6$ Hz, H-4), 8.13 (d, 2H, $J = 8.8$ Hz, H-3' and H-5'), 8.44 (d, 2H, $J = 8.8$ Hz, H-2' and H-6'), 11.42 (s, 1H, NH Isatin), 14.00 (br s, 1H, NH Hydrazone). ^{13}C NMR (100 MHz, $\text{DMSO}-d_6$): 111.78, 115.93, 120.05, 121.66, 124.03, 124.72, 127.60, 130.49, 133.68, 138.14, 143.18, 149.85, 163.44. MS (m/z , %): 310 (M^+ , 23), 282 (13), 264 (16), 236 (26), 211 (15), 183 (23), 160 (100), 132 (95), 120 (24), 104 (95), 92 (30), 76 (67), 57 (87). Anal. Calcd for $\text{C}_{15}\text{H}_{10}\text{N}_4\text{O}_4$: C, 58.07; H, 3.25; N, 18.06. Found: C, 57.88; H, 3.21; N, 18.12.

(Z)-N'-(1-methyl-2-oxoindolin-3-ylidene)benzohydrazide (**6a**). Yellow solid; Yield: 73%; m.p.: 183–185 °C; IR (KBr, cm^{-1}): 3436, 3108, 2956, 1698, 1542, 1043; ^1H NMR (400 MHz, CDCl_3) δ : 3.34 (s, 3H, CH_3), 6.93 (d, 1H, $J = 7.6$ Hz, H-7), 7.19 (t, 1H, $J = 7.6$ Hz, H-5), 7.44 (dt, 1H, $J = 7.2$ and 1.2 Hz, H-6), 7.55 (t, 2H, $J = 7.6$ Hz, H-3' and H-5'), 7.63 (t, 1H, $J = 7.2$ Hz, H-4'), 7.88 (d, 1H, $J = 7.2$ Hz, H-4), 8.04 (d, 2H, $J = 8.5$ Hz, H-2' and H-6'), 14.11 (br s, 1H, NH Hydrazone). ^{13}C NMR (100 MHz, $\text{DMSO}-d_6$): 26.25, 110.63, 115.30, 119.36, 121.33, 123.88, 124.73, 126.47, 129.55, 132.59, 138.08, 144.49, 162.15. MS (m/z , %): 279 (M^+ , 23), 183 (10), 174 (70), 146 (48), 117 (22), 105 (92), 91 (42), 81 (44), 77 (96), 69 (100). Anal. Calcd for $\text{C}_{16}\text{H}_{13}\text{N}_3\text{O}_2$: C, 68.81; H, 4.69; N, 15.05. Found: C, 69.02; H, 4.91; N, 15.18.

(Z)-4-hydroxy-N'-(1-methyl-2-oxoindolin-3-ylidene)benzohydrazide (**6b**). Yellow solid; Yield: 91%; m.p.: 318–320 °C; IR (KBr, cm^{-1}): 3406, 3179, 3116, 2932, 1685, 1543, 1183, 1042; ^1H NMR (400 MHz, $\text{DMSO}-d_6$) δ : 3.25 (s, 3H, CH_3), 6.96 (d, 2H, $J = 8.8$ Hz, H-3' and H-5'), 7.17 (d, 1H, $J = 8.0$ Hz, H-7), 7.18 (t, 1H, $J = 6.8$ Hz, H-5), 7.48 (dt, 1H, $J = 8.2$ and 1.2 Hz, H-6), 7.63 (dd, 1H, $J = 8.0$ and 1.2 Hz, H-4), 7.79 (d, 2H, $J = 8.8$ Hz, H-2' and H-6'), 10.44 (s, 1H, OH), 13.83 (s, 1H, NH Hydrazone). ^{13}C NMR (100 MHz, $\text{DMSO}-d_6$): 26.15, 110.43, 116.28, 119.68, 120.88, 122.79, 123.70, 130.12, 131.26, 131.87, 136.92, 143.91, 161.71, 162.26. MS (m/z , %): 295 (M^+ , 37), 267 (10), 173 (81), 146 (68), 117 (59), 93 (100), 77 (30), 65 (84). Anal. Calcd for $\text{C}_{16}\text{H}_{13}\text{N}_3\text{O}_3$: C, 65.08; H, 4.44; N, 14.23. Found: C, 65.11; H, 4.27; N, 14.28.

(Z)-4-methyl-N'-(1-methyl-2-oxoindolin-3-ylidene)benzohydrazide (**6c**). Yellow solid; Yield: 80%; m.p.: 203–205 °C; IR (KBr, cm^{-1}): 3436, 3120, 2922, 1708, 1534, 1038; ^1H NMR (400 MHz, CDCl_3) δ : 2.46 (s, 3H, CH_3), 3.33 (s, 3H, CH_3), 6.92 (d, 1H, $J = 8.0$ Hz, H-7), 7.18 (t, 1H, $J = 7.6$ Hz, H-5), 7.34 (d, 2H, $J = 8.0$ Hz, H-3' and H-5'), 7.43 (dt, 1H, $J = 7.6$ and 1.2 Hz, H-6), 7.89 (d, 1H, $J = 7.6$ Hz, H-4), 7.94 (d, 2H, $J = 8.4$ Hz, H-2' and H-6'), 14.06 (br s, 1H, NH Hydrazone). ^{13}C NMR (100 MHz, $\text{DMSO}-d_6$): 21.57, 26.18, 110.49, 119.58, 121.03, 123.75, 127.88, 129.57, 130.19, 132.10, 143.78, 144.08, 161.69. MS (m/z , %): 293 (M^+ , 10), 183 (7), 173 (18), 146 (19), 119 (91), 91 (100), 65 (40), 43 (15). Anal. Calcd for $\text{C}_{17}\text{H}_{15}\text{N}_3\text{O}_2$: C, 69.61; H, 5.15; N, 14.33. Found: C, 69.73; H, 5.11; N, 14.06.

(Z)-4-chloro-N'-(1-methyl-2-oxoindolin-3-ylidene)benzohydrazide (**6d**). Yellow solid; Yield: 79%; m.p.: 278–280 °C; IR (KBr, cm^{-1}): 3450, 3112, 2944, 1703, 1533, 1013; ^1H NMR (400 MHz, CDCl_3) δ : 3.33 (s, 3H, CH_3), 6.93 (d, 1H, $J = 7.6$ Hz, H-7), 7.19 (t, 1H, $J = 7.6$ Hz, H-5), 7.44 (dt, 1H, $J = 7.6$ and 1.2 Hz, H-6), 7.52 (d, 2H, $J = 8.4$ Hz, H-3' and

H-5'), 7.87 (d, 1H, $J = 7.6$ Hz, H-4), 7.97 (d, 2H, $J = 8.4$ Hz, H-2' and H-6'), 14.12 (br s, 1H, NH). ^{13}C NMR (100 MHz, $\text{DMSO}-d_6$): 26.18, 110.54, 119.44, 121.14, 123.79, 129.76, 131.17, 132.30, 138.22, 144.19, 161.62. MS (m/z , %): 313 (M^+ , 52), 174 (70), 146 (68), 139 (100), 118 (38), 111 (91), 91 (56), 75 (53). Anal. Calcd for $\text{C}_{16}\text{H}_{12}\text{ClN}_3\text{O}_2$: C, 61.25; H, 3.86; N, 13.39. Found: C, 61.23; H, 3.92; N, 13.20.

(Z)-N'-(1-methyl-2-oxoindolin-3-ylidene)isonicotinohydrazide (**6e**). Yellow solid; Yield: 83%; m.p.: 223–225 °C; IR (KBr, cm^{-1}): 3434, 3113, 2944, 1699, 1519, 1041; ^1H NMR (400 MHz, CDCl_3) δ : 3.33 (s, 3H, CH_3), 6.94 (d, 1H, $J = 7.6$ Hz, H-7), 7.20 (t, 1H, $J = 7.6$ Hz, H-5), 7.46 (t, 1H, $J = 8.0$ Hz, H-6), 7.85 (d, 2H, $J = 5.2$ Hz, H-2' and H-6'), 7.88 (d, 1H, $J = 7.6$ Hz, H-4), 8.87 (d, 2H, $J = 5.2$ Hz, H-3' and H-5'), 14.23 (s, 1H, NH Hydrazone). ^{13}C NMR (100 MHz, $\text{DMSO}-d_6$): 26.21, 110.61, 119.28, 121.32, 121.49, 123.86, 132.58, 139.53, 144.38, 151.42, 161.56. MS (m/z , %): 280 (M^+ , 28), 174 (56), 146 (97), 117 (45), 91 (100), 78 (97), 51 (95). Anal. Calcd for $\text{C}_{15}\text{H}_{12}\text{N}_4\text{O}_2$: C, 64.28; H, 4.32; N, 19.99. Found: C, 64.45; H, 4.36; N, 19.93.

4.2. Pharmacology

Pharmacological studies were fulfilled in the Toxicology and Pharmacology Research Laboratories of the Mazandaran University of Medical Sciences. All experiments were accomplished in accordance with the ethical standards and protocols approved by the Committee of Animal Experimentation of Mazandaran University of Medical Sciences, Sari, Iran (Ethics Code: IR.MAZUMS.REC.1396.3157). Dual Impedance Research Stimulator, ear electrodes, and Rotarod device were used for the anticonvulsant and neurotoxicity evaluations. Male Swiss albino mice with 20–25 g weight were used for *in vivo* studies. The animals were housed at 25 ± 2 °C and a 12 h light/dark cycle in standard Plexiglas cages with access to adequate water and food. The stock solutions of compounds were prepared in DMSO and each compound was administered as an i.p. injection at the required doses. The negative control groups were received the vehicle. Normal saline 0.9% was used to prepare the PTZ solution, and solution was kept at 4 °C during testing.

4.2.1. MES-induced seizure test

The animals were randomly divided into different treatment groups then test compounds were administrated i.p. in mice. 30 min later, mice were restrained for electrical stimulation and electrical seizures were induced by dual impedance research stimulator (Borj-Sanat, Iran) via ear clip electrodes, coated with an electrolyte solution. The alternating current of 50 mA (60 Hz) was delivered for 0.2 s to induce seizure in mice. After electrical stimulation, animals were instantly moved to a Plexiglas arena for behavioral observation. The negative control group was fully associated with the hind-limb tonic extension (HLTE). The reduction in the incidence of HLTE was recorded in the drug-treated mice [60].

4.2.2. PTZ-induced seizure test

At first, each animal group was treated with different doses of compounds **5a-e** and **6a-e**. After 30 min, a solution of PTZ (100 mg/kg) was injected i.p. and animals were kept in distinct cages and monitored for 0.5 h. The incidence of tonic-clonic convulsion and subsequently death following it was recorded for each animal in the group [60].

4.2.3. Acute neurotoxicity (Rotarod test)

The selected compound (**6e**, at the doses of 2.5, 5 and 10 mg/kg), diazepam (2 mg/kg, as reference drug) and DMSO (as control) were administered i.p. After administration (0.5, 1, 2, and 4 h), mice were placed on the rotating rod (6 rpm) and the time that the mice were able to maintain their balance on the rotating rod was recorded.

4.3. Docking simulation

Autodock Vina v1.2 has been utilized to study the binding mode of

our compounds with five famous molecular targets of antiepileptic agents, VGSCs, GABA_A, NMDA, AMPA and GABA-T. These studies were performed on the PDB code of 6D6T (GABA_A), 1FTL (AMPA), 5EKO (VGSCs), 1OHV (GABA-T), and 1PBQ (NMDA). The receptor structures were prepared by Molegro Molecular Viewer 2.5 (A CLC bio company, 2012). For preparation, water molecules were first removed and protein structure was protonated at physiological pH. On the other hand, to generate the lowest energy conformations of ligands, HyperChem v.8, with MM2 force field was used. For protein and ligand, Kollman and Gasteiger charges were computed respectively by AutoDock 4.2, and then docking study was performed with AutoDock Vina v1.2. Finally, Discovery Studio Visualizer v4.5 was used for visualizing ligand–protein interactions and generating 2D and 3D-images [61].

4.4. MTT cytotoxicity assay

SH-SY5Y and HepG2 cancer cell lines with a density of 1×10^4 cells/well, were cultured in 96-well plates for 24 h prior to treatment. After incubation time, cells were treated with different concentration of compounds **6a** and **6e**. After 48 h of treatment, 20 μ l MTT solution (5 mg/ml) was added to each well then incubation at 37 °C for 3–4 h. Subsequently, 200 μ l of DMSO was added to each well and the plates were shaken for 5 min. Finally, the optical absorption of samples was determined at 570 nm using a multi-well plate reader. Irinotecan and 5-Fluorouracil were used as reference drugs. The negative control group was untreated cells.

4.5. PPB determination

High-performance liquid chromatography was used with a PerkinElmer HPLC system (analytical reverse phase HPLC, Germany) to determine the PPB of compounds **6a** and **6e**. Sample (20 μ l) was injected into a C18 column (150 mm length, 3 mm inner diameter and 5 μ m particle size); maintained at 25 °C with an isocratic mobile phase (10% H₂O and 90% methanol) and a flow rate of 1 ml/min. The test compounds were detected at a wavelength of 274 nm. The retention times of compounds **6a** and **6e** were 3.37 and 3.38 min, respectively.

The stock solution (1 mM) of tested compounds **6a** and **6e** were prepared by dissolving an appropriate amount in methanol (HPLC grade). Secondary solution (100 μ M) was prepared through dilution of stock solution in the methanol, and then 20 μ l of them injected to the HPLC and its absorption was recorded by a UV detector. In the next step, 100 μ l of the stock solution (1 mM) of test compounds was added to a microtube containing 900 μ l of BSA (40 mg/ml, 6.06×10^{-4} M), then vortexed for 60 s, and the mixture was incubated at 37 °C for 45 min. Thereafter, 1000 μ l of TCA (trichloroacetic acid) solution (10% w/v) was added into the sample tube. The final mixture was subjected to centrifugation for 30 min (3000 rpm) at 37 °C. After addition of TCA to the mixture, the precipitated albumin and bonded molecules were separated by centrifugation. To estimate the percentage of protein binding, 20 μ l of supernatant solution was injected into the HPLC column, and the concentration of the free molecules (non-bonded to albumin) analyzed by HPLC chromatograph (PerkinElmer Corporation, Germany). Finally, the PPB rate of tested compounds was calculated by considering the ratio of bounded molecules to the BSA respect to the total.

4.6. Measurement of Log p

The measurement of Log P was conducted by analyzing with HPLC according to the previously reported method [62].

Declaration of Competing Interest

The authors declare that they have no known competing financial interests or personal relationships that could have appeared to influence

the work reported in this paper.

Acknowledgments

A part of this work was supported by a grant (No. 3157) from the Research Council of Mazandaran University of Medical Sciences, Sari, Iran.

Appendix A. Supplementary material

Supplementary data to this article can be found online at <https://doi.org/10.1016/j.bioorg.2021.104943>.

References

- [1] R.D. Thijs, R. Surges, T.J. O'Brien, J.W. Sander, Epilepsy in adults, *The Lancet* (2019).
- [2] S. Saxena, S. Li, Defeating epilepsy: A global public health commitment, *Epilepsia open*. 2 (2) (2017) 153–155.
- [3] I.E. Scheffer, S. Berkovic, G. Capovilla, M.B. Connolly, J. French, L. Guilhoto, et al., ILAE classification of the epilepsies: position paper of the ILAE Commission for Classification and Terminology, *Epilepsia*. 58 (4) (2017) 512–521.
- [4] P. Camfield, C. Camfield, Regression in children with epilepsy, *Neurosci. Biobehav. Rev.* 96 (2019) 210–218.
- [5] Z. Chen, M.J. Brodie, D. Liew, P. Kwan, Treatment outcomes in patients with newly diagnosed epilepsy treated with established and new antiepileptic drugs: a 30-year longitudinal cohort study, *JAMA Neurol.* 75 (3) (2018) 279–286.
- [6] G. Zaccara, E. Perucca, Interactions between antiepileptic drugs, and between antiepileptic drugs and other drugs, *Epileptic Disorders*. 16 (4) (2014) 409–431.
- [7] M. Bosak, A. Slowik, A. Iwańska, M. Lipińska, W. Turaj, Co-medication and potential drug interactions among patients with epilepsy, *Seizure*. 66 (2019) 47–52.
- [8] J. Woron, M. Siwek, Unwanted effects of psychotropic drug interactions with medicinal products and diet supplements containing plant extracts, *Psychiatr. Pol.* 52 (6) (2018) 983–996.
- [9] M. Bosak, K. Cyrancka, D. Dudek, M. Kowalik, P. Molek, A. Slowik, Psychiatric comorbidity in patients with epilepsy, *Epilepsy Behav.* 83 (2018) 207–211.
- [10] H.L. Zhu, J.B. Wan, Y.T. Wang, B.C. Li, C. Xiang, J. He, et al., Medicinal compounds with antiepileptic/anticonvulsant activities, *Epilepsia*. 55 (1) (2014) 3–16.
- [11] M. Bialer, Chemical properties of antiepileptic drugs (AEDs), *Adv. Drug Deliv. Rev.* 64 (10) (2012) 887–895.
- [12] M.N. Aboul-Enen, A.A. El-Azzouny, O.A.Y.A. Maklad Saleh, On chemical structures with potent antiepileptic/anticonvulsant profile, *Mini Rev. Med. Chem.* 12 (2012) 671–700.
- [13] C. Xie, L.-M. Tang, F.-N. Li, L.-P. Guan, C.-Y. Pan, S.-H. Wang, Structure-based design, synthesis, and anticonvulsant activity of isatin-1-N-phenylacetamide derivatives, *Med. Chem. Res.* 23 (5) (2014) 2161–2168.
- [14] P. Pakravan, S. Kashanian, M.M. Khodaei, F.J. Harding, Biochemical and pharmacological characterization of isatin and its derivatives: from structure to activity, *Pharmacol. Rep.* 65 (2) (2013) 313–335.
- [15] R.S. Cheke, S.D. Firke, R.R. Patil, S.B. ISATIN Bari, New hope against convulsion, *Cent. Nerv. Syst. Agents Med. Chem.* 18 (2018) 76–101.
- [16] M.R. Khajouei, A. Mohammadi-Farani, A. Moradi, A. Aliabadi, Synthesis and evaluation of anticonvulsant activity of (Z)-4-(2-oxoindolin-3-ylideneamino)-N-phenylbenzamide derivatives in mice, *Res. Pharm. Sci.* 13 (3) (2018) 262.
- [17] G. Saravanan, V. Alagarsamy, P. Dineshkumar, Anticonvulsant activity of novel 1-(morpholinomethyl)-3-substituted isatin derivatives, *Bulletin of Faculty of Pharmacy, Cairo University*, 2014, pp. 115–124.
- [18] O.Y. Voskoboinik, O.S. Kolomoets, I.S. Nosulenko, G.G. Berest, A.K. Bilyi, O. V. Karpenko, et al., Synthesis, Modification, and Anticonvulsant Activity of 3'-R1-Spiro [indoline-3, 6'-[1, 2, 4] triazino [2, 3-c] quinazolin]-2, 2' (7' H)-diones Derivatives, *J. Heterocycl. Chem.* 56 (5) (2019) 1605–1612.
- [19] A.P. Nikalje, A. Ansari, S. Bari, V. Ugale, Synthesis, Biological Activity, and Docking Study of Novel Isatin Coupled Thiazolidin-4-one Derivatives as Anticonvulsants, *Arch. Pharm.* 348 (6) (2015) 433–445.
- [20] S. Vogel, D. Kaufmann, M. Pojarová, C. Müller, T. Pfaller, S. Kühne, P.J. Bednarski, E. von Angerer, Aryl hydrazones of 2-phenylindole-3-carbaldehydes as novel antimitotic agents, *Bioorg. Med. Chem.* 16 (12) (2008) 6436–6447.
- [21] Y. Ozkay, Y. Tunali, H. Karaca, I. Işıkdağ, Antimicrobial activity and a SAR study of some novel benzimidazole derivatives bearing hydrazone moiety, *Eur. J. Med. Chem.* 45 (2010) 3293–3298.
- [22] I. Iliev, D. Kontrec, R. Detcheva, M. Georgieva, A. Balacheva, N. Galić, T. Pajpanova, Cancer cell growth inhibition by aroylhydrazone derivatives, *Biotechnol. Biotechnol. Equip.* 33 (1) (2019) 756–763.
- [23] A.A. Mohamed Eissa, G.A. Soliman, M.H. Khataibeh, Design, synthesis and anti-inflammatory activity of structurally simple anthranilic acid congeners devoid of ulcerogenic side effects, *Chem. Pharm. Bulletin (Tokyo)* 60 (2012) 1290–1300.
- [24] C.M. Leal, S.L. Pereira, A.E. Kümmerle, D.M. Leal, R. Tesch, C.M. de Sant'Anna, C. A. Fraga, E.J. Barreiro, R.T. Sudo, G. Zapata-Sudo, Antihypertensive profile of 2-thienyl-3,4-methylenedioxybenzoylhydrazone is mediated by activation of the A2A adenosine receptor, *Eur. J. Med. Chem.* 55 (2012) 49–57.

- [25] L.M. Lima, F.S. Frattani, J.L. Dos Santos, H.C. Castro, C.A. Fraga, R.B. Zingali, et al., Synthesis and anti-platelet activity of novel arylsulfonate – Acylhydrazone derivatives, designed as antithrombotic candidates, *Eur. J. Med. Chem.* 43 (2008) 348–356.
- [26] L. Dehestani, N. Ahangar, S.M. Hashemi, H. Irannejad, P.H. Masihi, A. Shakiba, et al., Design, synthesis, in vivo and in silico evaluation of phenacyl triazole hydrazones as new anticonvulsant agents, *Bioorg. Chem.* 78 (2018) 119–129.
- [27] V. Angelova, V. Karabeliov, P.A. Andreeva-Gateva, J. Tchekalarova, Recent developments of hydrazide/hydrazone derivatives and their analogs as anticonvulsant agents in animal models, *Drug Dev. Res.* 77 (7) (2016) 379–392.
- [28] L. Tripathi, R. Singh, J.P. Stables, Design & synthesis of N'-[substituted]pyridine-4-carbohydrazides as potential anticonvulsant agents, *Eur. J. Med. Chem.* 46 (2011) 509–518.
- [29] P. Kumar, B. Shrivastava, S.N. Pandeya, J.P. Stables, Design, synthesis and potential 6 Hz psychomotor seizure test activity of some novel 2-(substituted)-3-[substituted] amino} quinazolin-4 (3H)-one, *Eur. J. Med. Chem.* 46 (4) (2011) 1006–1018.
- [30] S.N. Pandeya, S. Smitha, J.P. Stables, Anticonvulsant and Sedative-Hypnotic Activities of N-Substituted Isatin Semicarbazones, *Archiv der Pharmazie A Int. J. Pharm. Med. Chem.* 335 (4) (2002) 129–134.
- [31] S. Emami, Z. Esmaili, G. Dehghan, M. Bahmani, S.M. Hashemi, H. Mirzaei, M. Shokrzadeh, S.E. Moradi, Acetophenone benzoylhydrazones as antioxidant agents: Synthesis, in vitro evaluation and structure-activity relationship studies, *Food Chem.* 268 (2018) 292–299.
- [32] L. Gupta, N. Sunduru, A. Verma, S. Srivastava, S. Gupta, N. Goyal, et al., Synthesis and biological evaluation of new [1, 2, 4] triazino [5, 6-b] indol-3-ylthio-1, 3, 5-triazines and [1, 2, 4] triazino [5, 6-b] indol-3-ylthio-pyrimidines against *Leishmania donovani*, *Eur. J. Med. Chem.* 45 (6) (2010) 2359–2365.
- [33] S. Tiwari, P. Pathak, R. Sagar, Efficient synthesis of new 2,3-dihydrooxazole-spirooxindoles hybrids as antimicrobial agents, *Bioorg. Med. Chem. Lett.* 26 (10) (2016) 2513–2516.
- [34] L. Somogyi, Transformation of isatin 3-acylhydrazones under acetylating conditions: Synthesis and structure elucidation of 1,5'-disubstituted 3'-acetylspiro [oxindole-3,2'-(1,3,4)oxadiazolines], *Bull. Chem. Soc. Jpn.* 74 (2001) 873–881.
- [35] J. Wang, D. Huang, K.H. Wang, X. Peng, Y. Su, Y. Hu, Y. Fu, Tin powder-promoted one-pot synthesis of 3-spiro-fused or 3,3'-disubstituted 2-oxindoles, *Org. Biomol. Chem.* 14 (40) (2016) 9533–9542.
- [36] P.E. Hansen, J. Spanget-Larsen, NMR and IR Investigations of Strong intramolecular hydrogen bonds, *Molecules* 22 (4) (2017) 552.
- [37] P.K. Sharma, S. Balwani, D. Mathur, S. Malhotra, B.K. Singh, A.K. Prasad, C. Len, E. V. Van der Eycken, B. Ghosh, N.G. Richards, V.S. Parmar, Synthesis and anti-inflammatory activity evaluation of novel triazolyl-isatin hybrids, *J. Enzyme Inhib. Med. Chem.* 31 (6) (2016) 1520–1526.
- [38] M.M. Castel-Branco, G.L. Alves, I.V. Figueiredo, A.C. Falcão, M.M. Caramona, The maximal electroshock seizure (MES) model in the preclinical assessment of potential new antiepileptic drugs, *Methods Find. Exp. Clin. Pharmacol.* 31 (2009) 101–106.
- [39] A. Dhir, Pentylene-tetrazol (PTZ) kindling model of epilepsy, *Curr. Protoc. Neurosci.* 2012; Chapter 9: Unit 9.37. <https://doi.org/10.1002/0471142301.nso937s58>.
- [40] D.W. Robertson, E. Beedle, R. Lawson, J.D. Leander, Imidazole anticonvulsants: structure-activity relationships of [(biphenylloxy) alkyl] imidazoles, *J. Med. Chem.* 30 (5) (1987) 939–943.
- [41] P.N. Patsalos, M. Zugman, C. Lake, A. James, N. Ratnaraj, J.W. Sander, Serum protein binding of 25 antiepileptic drugs in a routine clinical setting: A comparison of free non-protein-bound concentrations, *Epilepsia.* 58 (7) (2017) 1234–1243.
- [42] G.L. Trainor, The importance of plasma protein binding in drug discovery, *Expert Opin. Drug Discov.* 2 (1) (2007) 51–64.
- [43] A. Reimers, J.A. Berg, M.L. Burns, E. Brodtkorb, S.I. Johannessen, C.J. Landmark, Reference ranges for antiepileptic drugs revisited: a practical approach to establish national guidelines, *Drug Design Develop. Therapy* 12 (2018) 271.
- [44] R.E. Wang, L. Tian, Y.-H. Chang, A homogeneous fluorescent sensor for human serum albumin, *J. Pharm. Biomed. Anal.* 63 (2012) 165–169.
- [45] D. Chen, M. Zhao, W. Tan, Y. Li, X. Li, Y. Li, et al., Effects of intramolecular hydrogen bonds on lipophilicity, *Eur. J. Pharm. Sci.* 130 (2019) 100–106.
- [46] C.A. Lipinski, Lead-and drug-like compounds: the rule-of-five revolution, *Drug Discovery Today Technol.* 1 (4) (2004) 337–341.
- [47] H. van de Waterbeemd, G. Camenisch, G. Folkers, J.R. Chretien, O.A. Raevsky, Estimation of blood-brain barrier crossing of drugs using molecular size and shape, and H-bonding descriptors, *J. Drug Target.* 6 (2) (1998) 151–165.
- [48] P.D. Leeson, A.M. Davis, Time-related differences in the physical property profiles of oral drugs, *J. Med. Chem.* 47 (25) (2004) 6338–6348.
- [49] V.A. Ashwood, M.J. Field, D.C. Horwell, C. Julien-Larose, R.A. Lewthwaite, S. McCleary, et al., Utilization of an intramolecular hydrogen bond to increase the CNS penetration of an NK1 receptor antagonist, *J. Med. Chem.* 44 (14) (2001) 2276–2285.
- [50] D.F. Veber, S.R. Johnson, H.-Y. Cheng, B.R. Smith, K.W. Ward, K.D. Kopple, Molecular properties that influence the oral bioavailability of drug candidates, *J. Med. Chem.* 45 (12) (2002) 2615–2623.
- [51] J. Vidaurre, A. Gedela, S. Yarosz, Antiepileptic drugs and liver disease, *Pediatr. Neurol.* 77 (2017) 23–36.
- [52] H. Pajouhesh, G.R. Lenz, Medicinal chemical properties of successful central nervous system drugs, *NeuroRx.* 2 (4) (2005) 541–553.
- [53] X.-Y. Meng, H.-X. Zhang, M. Mezei, M. Cui, Molecular docking: a powerful approach for structure-based drug discovery, *Curr. Comput. Aided Drug Des.* 7 (2) (2011) 146–157.
- [54] O. Trott, A.J. Olson, AutoDock Vina: improving the speed and accuracy of docking with a new scoring function, efficient optimization, and multithreading, *J. Comput. Chem.* 31 (2) (2010) 455–461.
- [55] M.F. Acar, S. Sari, S. Dalkara, Synthesis, in vivo anticonvulsant testing, and molecular modeling studies of new nafimidone derivatives, *Drug Dev. Res.* (2019).
- [56] S.M. Landge, E. Tkatchouk, D. Benítez, D.A. Lanfranchi, M. Elhabiri, W. A. Goddard, I. Aprahamian, Isomerization mechanism in hydrazone-based rotary switches: lateral shift, rotation, or tautomerization? *J. Am. Chem. Soc.* 133 (2011) 9812–9823.
- [57] E.S. Yuen, I.F. Trocóniz, Can pentylene-tetrazole and maximal electroshock rodent seizure models quantitatively predict antiepileptic efficacy in humans? *Seizure.* 24 (2015) 21–27.
- [58] W. Löscher, D. Hönack, C.P. Fassbender, B. Nolting, The role of technical, biological and pharmacological factors in the laboratory evaluation of anticonvulsant drugs, III. Pentylene-tetrazole seizure models. *Epilepsy research.* 8 (3) (1991) 171–189.
- [59] K. Unverferth, J. Engel, N. Höfgen, A. Rostock, R. Günther, H.-J. Lankau, et al., Synthesis, anticonvulsant activity, and structure– activity relationships of sodium channel blocking 3-aminopyrroles, *J. Med. Chem.* 41 (1) (1998) 63–73.
- [60] N. Ahangar, A. Ayati, E. Alipour, A. Pashapour, A. Foroumadi, S. Emami, 1-[(2-arylthiazol-4-yl)methyl]azoles as a new class of anticonvulsants: design, synthesis, in vivo screening, and in silico drug-like properties, *Chem. Biol. Drug Des.* 78 (2011) 844–852.
- [61] H. Irannejad, H. Nadri, N. Naderi, S.N. Rezaeian, N. Zafari, A. Foroumadi, et al., Anticonvulsant activity of 1, 2, 4-triazine derivatives with pyridyl side chain: synthesis, biological, and computational study, *Med. Chem. Res.* 24 (6) (2015) 2505–2513.
- [62] S. Molavi-pordanjani, S. Emami, A. Mardanshahi, F.T. Amiri, Z. Noaparast, S. J. Hosseini-mehr, Novel ^{99m}Tc-2-arylimidazo [2, 1-b] benzothiazole derivatives as SPECT imaging agents for amyloid-β plaques, *Eur. J. Med. Chem.* 175 (2019) 149–161.